

L-H confinement transitions and predator-prey model; intrinsic rotation

Lecture by Professor P.H. Diamond,
notes by A.R. Knyazev

1 Predator $|\phi_q|^2$ prey $\langle N \rangle$ model for drift wave / zonal flow feedback

This section illustrates how the dynamics of the interplay between the drift wave turbulence and zonal flows can be understood from the perspective of ecological models. Recall that the wave kinetic equation for the drift wave action density

$$\frac{\partial \langle N \rangle}{\partial t} - \frac{\partial}{\partial k_r} D_k \frac{\partial}{\partial k_r} \langle N \rangle = \gamma \langle N \rangle - \frac{\Delta \omega_n}{N_0} \langle N \rangle^2 \quad (1)$$

implies the drift wave energy equation

$$\frac{\partial \langle \mathcal{E} \rangle}{\partial t} = - \int d^3 k \left(\frac{\partial \omega_k}{\partial k_r} \right) D_{k_r} \frac{\partial \langle N \rangle}{\partial k_r} + \int d^3 k \omega \langle C(N) \rangle + \text{surface term}, \quad (2)$$

Notably, the k -radial space diffusion in 2 is quadratic in the sheering field (with a negative sign),

$$D_{k_r} \sim O(\langle \tilde{V}^2 \rangle). \quad (3)$$

meaning it is determined by the sheering field's energy. The second RHS term in (2) accounts for growth and not-action conserving scattering that gives damping,

$$\int d^3 k \omega \langle C(N) \rangle \sim \gamma \langle \varepsilon \rangle - \frac{1}{\tau_{NL}} \langle \varepsilon \rangle^2. \quad (4)$$

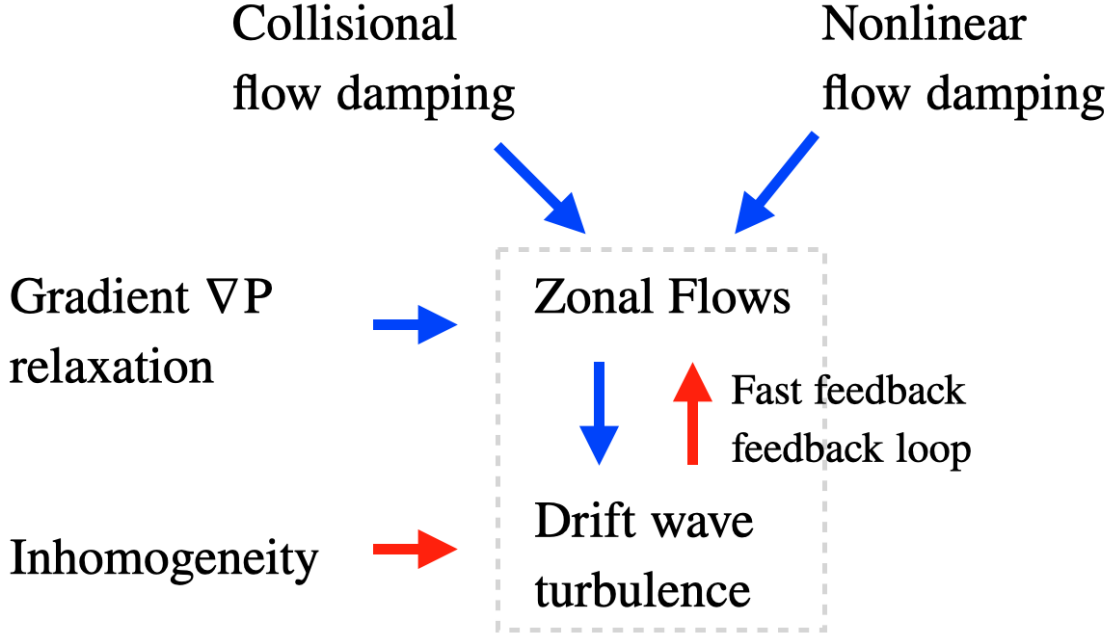
Meanwhile, expression for the energy of the $E \times B$ flow, i.e. $|\phi_q|^2$, is

$$\frac{\partial |\phi_q|^2}{\partial t} = \Gamma_q \left[\frac{\partial \langle N \rangle}{\partial k_r} \right] |\phi_q|^2 - \gamma_d |\phi_q|^2, \quad (5)$$

where γ_d is the zonal flow damping term, and the growth coefficient is related to the gradient of the wave population N in k space. The $|\Gamma_q |\phi_q|^2|$ is quadratic in shear with a positive sign. The energy flow in the resulting coupled system (2,5) has a feedback loop shown below, and the evolution of a system can be viewed as a predator-prey model between the drift wave action density $\langle N \rangle$ and the zonal flow $|\phi_q|^2$:

$$\frac{\partial \langle N \rangle}{\partial t} - \frac{\partial}{\partial k_r} D_k \frac{\partial}{\partial k_r} \langle N \rangle = \gamma_k \langle N \rangle - \frac{\Delta \omega_k}{N_0} \langle N \rangle^2, \quad (6)$$

$$\frac{\partial}{\partial t} |\phi_q|^2 = \Gamma_q \left[\frac{\partial \langle N \rangle}{\partial k_r} \right] |\phi_q|^2 - \gamma_d |\phi_q|^2 - \gamma_{NL} [|\phi_q|^2] |\phi_q|^2 \quad (7)$$



Reducing the system further to the mean-field predator-prey model,

$$\frac{\partial}{\partial t} N = \gamma N - \alpha V^2 N - \Delta\omega N^2, \quad (8)$$

$$\frac{\partial}{\partial t} V^2 = \alpha N V^2 - \gamma_d V^2 - \gamma_{NL} (V^2) V^2, \quad (9)$$

one can recover the phase portrait of the system (8,9) by classifying the fixed points. Neglecting the nonlinear damping $\gamma_{NL} = 0$, the non-trivial stationary points are

$$N = \frac{\gamma}{\Delta\omega}, \quad V^2 = 0, \quad \text{and} \quad N = \frac{\gamma_d}{\alpha}, \quad V^2 = -\frac{-\alpha\gamma + \gamma_d\Delta\omega}{\alpha^2}, \quad (10)$$

hence, notably, in presence of flow $V^2 > 0$, there is a stable saddle point with drift wave intensity is proportional to flow damping. The finite flow $V^2 > 0$ requirements sets the threshold on the grow rate γ , capturing the phenomenology of improved confinement threshold, namely: increase of energy increases the growth but does not increase the fluctuations because the energy goes into the flow. Enough growth (i.e. critical power threshold P_{th}) is needed to drive the flow against the damping. Without the residual nonlinear damping, the saddle becomes a center point, and phase trajectories satisfy

$$\frac{\gamma_d}{\gamma} \left(\frac{\alpha N}{\gamma_d} - \ln \frac{\alpha N}{\gamma_d} \right) + \frac{\alpha V^2}{\gamma} - \ln \frac{\alpha V^2}{\gamma} = const. \quad (11)$$

Initial zonal modes originate from incoherent drift wave beats, i.e. the beating of different modes (for example, \tilde{V}_{-k} and $\nabla^2 \tilde{\phi}_{k+q}$) will put the noise into the zonal mode:

$$\frac{\partial}{\partial t} (\nabla_{\perp}^2 \phi)_q \sim -(\tilde{V} \nabla \nabla^2 \tilde{\phi})_q. \quad (12)$$

Equation (12) is identical to the Langevin equation with the coherence time of the noise τ_{cq} set by the coherence time of stochastically driven Zonal Flow field (the correlation time of the vorticity flux $\langle \Gamma_{\nabla^2\phi} \Gamma_{\nabla^2\phi} \rangle$),

$$\frac{\partial}{\partial t} \langle (\nabla^2 \tilde{\phi})^2 \rangle \sim \sum_q (\tilde{\mathbf{V}} \cdot \nabla \nabla^2 \tilde{\phi})_q \tau_{cq} (\tilde{\mathbf{V}} \cdot \nabla \nabla^2 \tilde{\phi})_q \quad (13)$$

Also analogous to the Langevin equation for Brownian motion, the intensity of the zonal vorticity will grow linearly in time,

$$\langle (\nabla^2 \tilde{\phi}) \rangle \sim Dt. \quad (14)$$

Adding the noise term to the zonal mode growth equation allows for modulationally stable systems that still drive zonal flows.

1.0.1 Impact of geometry

Switching from cylindrical to toroidal geometry can increase the screening length and inertia of zonal flows. Specifically, since the divergence of polarization current is related to the vorticity evolution,

$$\nabla \cdot J_{\text{pol}} \sim \frac{d}{dt} \rho_s \nabla^2 \phi, \quad (15)$$

the impact of toroidicity is to modify the length scale due to particle trapping effects. The trapping effects occur at sufficiently low collisionality ν_* and increase the length scale from Larmour radius i to banana with

$$\delta r \sim v_D \tau_D \sim \frac{\rho_i v_{\tau i}}{R} \frac{Rq}{v_{\tau i} \sqrt{\epsilon}} \sim \sqrt{\epsilon} \rho_{\theta i}, \quad (16)$$

where $\rho_{\theta i}$ is the poloidal gyroradius. Relevance of particle trapping implies that the zonal flow response in toroidal geometry depends on collisionality ν_* , with Pfirsch-Schluter regime $\nu_* \gg \epsilon^{-3/2}$ recovering the cylindrical geometry results.

1.0.2 On mechanisms of ZF damping

In the Banana and Plateu regimes, the ZF are dumped by the friction between the bananas of the trapped particles and the flow. This collisional flow dumping mechanism is scale-invariant. In Pfirsch Schluter regime, the flow damping is related to magnetic pumping, i.e. the viscous dissipation caused by the need to compress a fluid element in order to move it from the weak field side to the strong field. The relative importance between viscosity νk^2 and damping $D_0 k^2$ depends on scale since $\nu k_r^2 \rightarrow 0$ for large k_r . Another scale-independent flow dumping mechanism is neutral friction due to charge exchange, which can be important for zonal flows at the edge and relevant to L-H transition. For sufficiently strong flows, the quasilinear theory calculation for the flux vorticity equation

$$\partial_t \langle \nabla_{\perp}^2 \phi \rangle = \partial_r \langle \tilde{v} \nabla_{\perp}^2 \tilde{\phi} \rangle + \text{lin. damping} \quad (17)$$

reveals a possibility for a wave flow resonance,

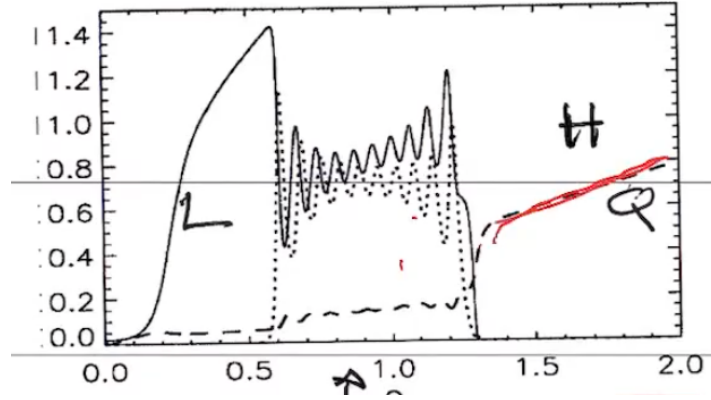
$$\nabla_{\perp}^2 \tilde{\phi} = -\frac{\tilde{v}_r \partial_r \langle \tilde{v}_r^2 \phi \rangle}{-i(\omega - k_{\theta} v_E)} + \frac{\alpha \tilde{h}}{-i(\omega - k_{\theta} v_{\theta})}, \quad (18)$$

resulting in a turbulent diffusion of vorticity

$$\langle \tilde{v} \nabla_{\perp}^2 \tilde{\phi} \rangle = -\sum_k |\tilde{v}_{rk}|^2 \Pi \delta(\omega - k_{\theta} v_E) \partial_r \langle \nabla_r^2 \phi \rangle + \dots \quad (19)$$

The effect of wave flow resonance gets stronger as the zonal flow grows, and provides another collisionless damping mechanism.

The predator-prey model can recover additional phenomenology of L-H transition by considering multiple predators. For instance, having three coupled equations for the energy (solid curve), zonal flow (dotted curve), and mean pressure gradient (dashed curve)



$$\partial_t \varepsilon = \varepsilon N - a_1 \varepsilon^2 - a_2 V^2 \varepsilon - a_3 V_{ZF}^2 \varepsilon, \quad (20)$$

$$\partial_t V_{ZF} = b_1 \frac{\varepsilon V_{ZF}}{1 + b_2 V^2} - b_3 V_{ZF}, \quad (21)$$

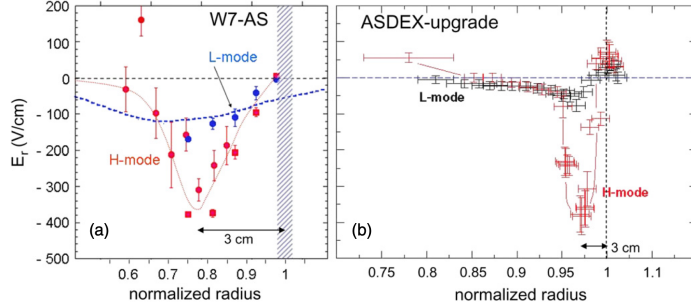
$$\partial_t N = -c_1 \varepsilon N - c_2 N + Q. \quad (22)$$

allows capturing the phenomenology of the transition phase. In (20-22), the pressure gradient is contributing to transport and damping the turbulence but is also driving it (replaces the growth rate).

2 L-H transition

The transition between regimes of low (L-mode) and improved (H-mode) confinement occurs as a bifurcation known as L-H transition. The mechanism of L-H transition is the radial decorrelation of turbulence by radially sheared $E \times B$ flows, as illustrated via predator-prey models in the previous section. (Although other possible LH transition mechanisms have also been proposed, such as the orbit loss mechanism). Due to the popularity of the improved confinement regime, conditions for L-H transition and the underlying physics are being studied. Important properties of L-H transition are listed below.

- Steepening of the edge gradient
- Pedestal formation
- Drop of fluctuations at low k (high k transport persists)
- Increase in $E \times B$ shear and formation of $\langle E_r \rangle$ well with two strong $E \times B$ shear layers on each side of the well, suppressing the turbulence. The transport barrier can develop on either the inner or outer layer of the well.



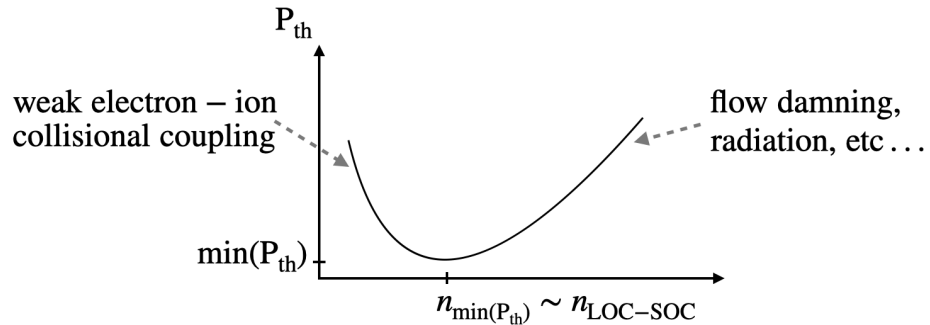
- Transition occurs at some power threshold P_{th} .
 - The mechanism of heating the plasma does not matter.
 - The power threshold scales with the density and toroidal field,

$$P_{th} \sim 0.049 B_T^{0.8} n_e^{0.72} S^{0.94}, \quad (23)$$

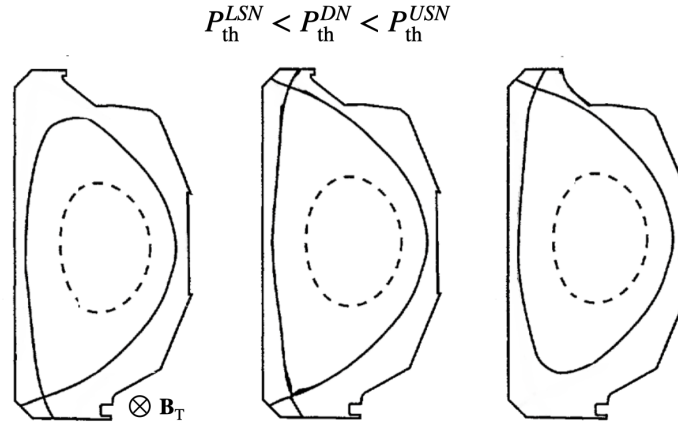
although experiments show that there is a minimum $n_{\min(P_{th})}$ in density dependence of P_{th} occurring near the LOC-SOC transition density. The similarity of $n_{\min(P_{th})}$ and $n_{LOC-SOC}$ is explained by the fact that both are related to ion energy transport in Ohmically heated plasmas, which is particularly relevant at lower densities. Collisional ion-electron energy coupling is quadratic in density

$$n\nu_e(T_e - T_i) \propto n^2, \quad (24)$$

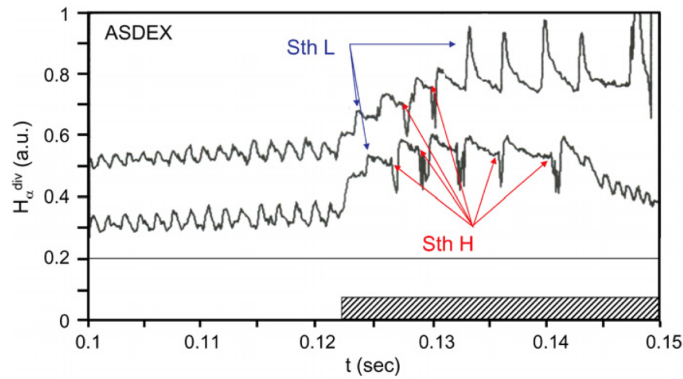
and so at low densities most of the energy is wasted into electrons instead of building a sufficient ion pressure gradient ∇P_i for the $L - H$ transition.



- the “ ∇B drift” asymmetry. Assuming the toroidal field is into the plane, the lower single null LSN has a lower Power threshold than the higher single null. Somewhere in the middle is the double null.



- Critical transition condition is local and resides at the plasma edge, as evidenced by L-H transitions triggered by sawteeth during L-mode discharge at power just below the transition threshold $P < P_{th}$,



- L-H hysteresis in power threshold. The power to go up is different from the power to come back $P_{LH} > P_{HL}$. The hysteresis phenomenon is still poorly understood because it is hard to isolate from ELMs.

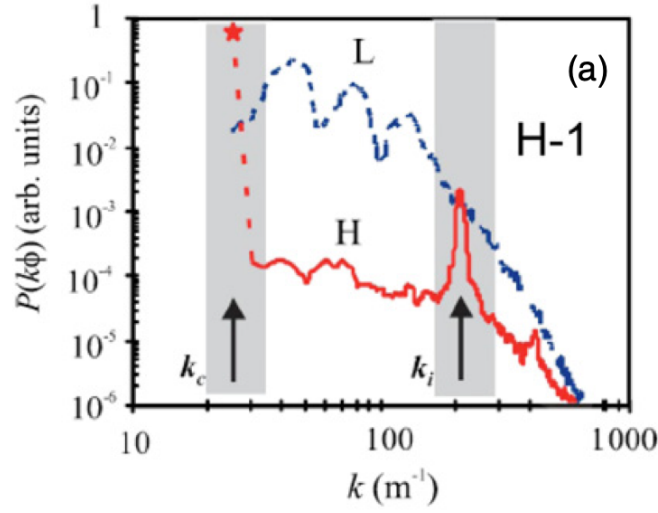
One of the ITER ideas is to make the transition at low density and increase density, relying on hysteresis to keep you in H mode

- The power threshold in tokamaks is different for different isotopes; for example, P_{th} in D is lower than H due to lower transport in D -plasmas. For stellarators, the power threshold is independent of the isotope.
- Although the H-mode was first discovered on tokamaks (ASDEX), it has since been demonstrated on stellarators (W7-AS) as well.
- Occurs in both limiter and diverted plasmas, although has not yet been shown in experiments with an outside limiter.

2.1 Relation to the inverse cascade

In a strict sense, an inverse cascade is a continuous transfer, i.e., flow in scale space. This should be contrasted with discrete scale interaction (energy cascades

from drift waves at large k to Zonal Flows at small k). This nonlocal transfer in k space allows to avoid the development of broadband turbulence and improves confinement.

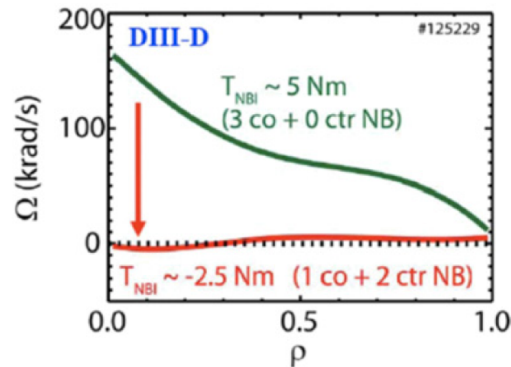


3 Momentum transport and intrinsic rotation

Development of Charge Exchange Recombination Spectroscopy in the late '80s enabled experimental measurement of toroidal velocity and temperature profiles in tokamaks. Subsequent studies of momentum transport inferred a non-diffusive momentum flux component and observed intrinsic rotation in H-mode plasmas. Particularly notable was the plasma rotation observed in ICRF heated tokamaks since it occurred in the absence of external torque from neutral beams.

Although momentum carried by ICRF waves was investigated as a possible external source, experiments on Ohmically heated tokamaks with $P_{OH} = P_{RF}$ matched the ICRF tokamak results and disproved the wave momentum scenario. As ICRF generates a high energy tail, matching of results for $P_{OH} = P_{RF}$ also suggested that orbit loss does not explain the effect.

Meanwhile, the presence of intrinsic torque was demonstrated in the counter-NBI experiments:



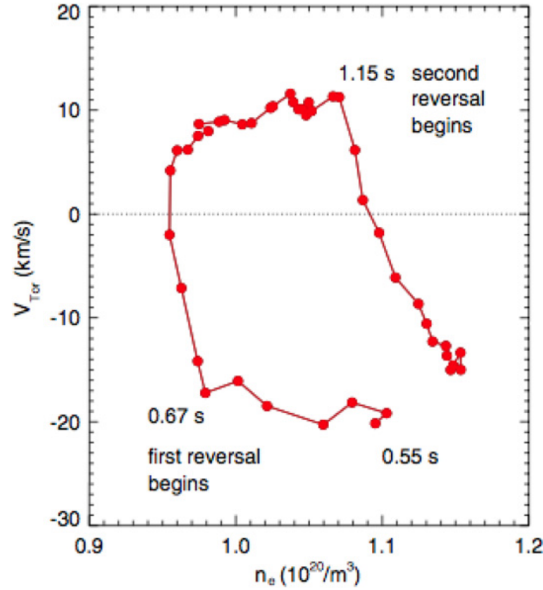
Intrinsic rotation speed is subsonic, but it is nevertheless significant. Associated sheared toroidal rotation improves confinement by contributing to the electric field

$$\langle E \rangle = \frac{\nabla P}{n} + \langle v \rangle \times B, \quad (25)$$

and helping to stabilize resistive wall modes (“kinks”). Early studies of intrinsic rotation produced a “Rice Scaling” that related the increments of rotation speed ΔV_ϕ to the ratio between the increments in plasma energy content ΔW at the L-H transition and the current I_p ,

$$\Delta V_\phi \approx \frac{\Delta W}{I_p}. \quad (26)$$

Another important example of intrinsic rotation is the momentum transport bifurcations occurring at the LOC-SOC transition, i.e. the flip of rotation profile as the density passes the $n_{\text{LOC-SOC}}$. Subsequent decrease in density results in a backflip, although a hysteresis is present:



Transition from SOC to IOC results in another flip, recovering the rotation direction from LOC regime. Because the SOC and IOC differ in the type of turbulence, this points to the relation between the nature of turbulence and intrinsic rotation. Shortly after the early experiments suggested $\chi_\phi \sim \chi_i$, it was recognised that diffusion alone is not sufficient to explain the change in profiles, and so the momentum flux should also contain a momentum pinch ($V < 0$) term:

$$\Pi = -\chi_\phi \frac{\partial \langle v_\phi \rangle}{\partial r} + V(r) \langle V_\phi \rangle. \quad (27)$$

The pinch by itself, however, is still not sufficient to explain the intrinsic rotation, which leads to the addition of a non-diffusive part of the Reynolds stress, i.e. residual stress:

$$\Pi = -\chi_\phi \frac{\partial \langle v_\phi \rangle}{\partial r} + V(r) \langle V_\phi \rangle + \Pi_{\text{resid}}, \quad (28)$$

where

$$\Pi_{\text{resid}} = nm_i [\langle \tilde{v}_{E,r} \tilde{v}_{||} \rangle + \langle \frac{c}{B} \tilde{E}_r \frac{c}{B} \tilde{E}_{||} \rangle - \frac{B_\theta}{B_T} \langle \tilde{v}_{E,r} \tilde{v}_\theta \rangle]. \quad (29)$$

The presence of Π_{resid} explains the spin-up of plasma

$$\frac{\partial}{\partial t} \int dr \langle V_\phi \rangle = -\Pi_{\text{resid}}|_0^{\text{boundary}}, \quad (30)$$

and points at the importance of the boundary. Calculating the parallel Reynolds stress for ITG modes

$$\frac{\partial}{\partial t} \tilde{v}_{||k} + \tilde{v}_{||k} = -\tilde{v}_{r_k} \frac{\partial \langle v_{||} \rangle}{\partial r} - \frac{ik_{||}}{\rho} \tilde{p}_{ki} + \dots, \quad (31)$$

$$\frac{\partial \tilde{p}_{ki}}{\partial t} + \frac{\tilde{p}}{\tau_{ck}} = -\tilde{v}_r \frac{\partial \langle p \rangle}{\partial r} - p_0 ik_{||} \hat{v}_{||k} \quad (32)$$

shows that the intrinsic rotation is driven by the ion pressure gradient

$$\Pi_{\text{resid}} \sim \sum_k \langle \tilde{v}_r^2 \rangle_k (\dots) \frac{\partial \langle p_i \rangle}{\partial r}. \quad (33)$$

Notably, in Reynolds stress

$$\langle \tilde{v}_r \tilde{v}_{||} \rangle = -\chi_\phi \frac{\partial \langle v \rangle}{\partial r} + d_{\text{resid}} \frac{\partial \langle p \rangle}{\partial r} \quad (34)$$

the d_{resid} is proportional to the odd spectral moment,

$$d_{\text{resid}} \sim \sum (\dots) k_{||} |\phi_k|^2, \quad (35)$$

implying that nonzero d_{resid} requires symmetry breaking, similar to the necessity for reflectional symmetry breaking in the mean-field theory of the turbulent magnetic dynamo.

Multiple mechanisms for symmetry breaking exist, some of the simpler ones being the shift of the spectrum due to $E \times B$ shear, yielding $\langle k_{||} \rangle$ and hence finite $\langle k_\theta k_{||} \rangle$. Somewhat more generally, the symmetry breaking in $\langle k_\theta k_{||} \rangle$ is also produced due to spectral dispersion with intensity gradient I' ,

